

# Study of Hopf bifurcations in a simple power system model

Juan Li and Vaithianathan Venkatasubramanian  
School of Electrical Engineering and Computer Science  
Washington State University  
Pullman, WA 99164-2752

**Abstract:** This paper studies the occurrence of Hopf bifurcations in a simple single-machine-infinite-bus (SMIB) power system model. Our interest is primarily on the subcritical or supercritical nature of the Hopf bifurcations under variations in operating parameters. We observe that the Hopf bifurcations are mostly subcritical. When the exciter control is a fast high gain control and when the Thevenin equivalent transmission line impedance is high, the Hopf bifurcation can become supercritical leading to birth of stable limit cycles. Two degenerate bifurcations namely, one related to double zero eigenvalues, and the other related to Hopf normal form coefficient becoming zero, give rise to homoclinic orbits and nested limit cycles respectively.

**Key words:** power system dynamics, bifurcations, power system stability.

## 1. Introduction

Under parametric variations, the phase portrait of a dynamical system undergoes qualitative changes at bifurcation points. When the changes occur around equilibrium points, the bifurcations are local and there exist well-established tools in bifurcation theory for analyzing the local bifurcations in a hierarchical fashion. Roughly speaking, when all the qualitative changes in the phase portrait near the bifurcation point can be characterized by variation of one parameter, the bifurcation is said to be of codimension one bifurcation. On the other hand, when the qualitative changes in the phase portrait can only be characterized by variation of two parameters, the bifurcation is of codimension two.

For smooth systems, Hopf bifurcations and saddle node bifurcations are the “typically” encountered codimension one bifurcations. When the system Jacobian has a simple pair of purely imaginary eigenvalues and no other zero real part eigenvalues, a Hopf bifurcation (denoted  $B_H$ ) occurs. Hopf bifurcation Theorem [1,2] then predicts the existence of limit cycles near the bifurcation point under some transversality conditions. The stability of the limit cycles depend on the nonlinear terms and specifically on the sign of a cubic normal form coefficient that is usually denoted “ $a$ ” [1,2]. When  $a$  is negative, the Hopf bifurcation is supercritical and when  $a$  is positive, the bifurcation is subcritical. Supercritical and subcritical Hopf bifurcations lead to birth of stable and unstable limit cycles respectively. When the system Jacobian has a simple zero eigenvalue and no other zero real part eigenvalues, a saddle node bifurcation (denoted  $B_{SN}$ ) occurs under certain transversality conditions. Saddle node Theorem then proves the annihilation of the equilibrium point at a saddle node bifurcation. In summary, Hopf bifurcations are

used to locate birth of limit cycles in a nonlinear system and saddle node bifurcations stand as static limit type boundaries where equilibrium points disappear. Hopf and saddle node bifurcations have been studied extensively in the context of power system dynamics (e.g. [3,6]).

When the operating parameters are near a codimension two bifurcation, the phase portraits may be richer in nonlinear phenomena. In this paper, we study two different codimension two bifurcations by phase portraits. At the first denoted a double zero bifurcation (denoted  $B_{DZ}$ ), the system Jacobian has couple of zero eigenvalues and no other zero real part eigenvalues. Double zero bifurcations arise at intersections of saddle node and Hopf bifurcations. Homoclinic orbit which is a closed trajectory connecting an equilibrium to itself, is of interest in the context of complicated system behavior. Homoclinic orbits are difficult to locate in general. Whereas, they are born at double zero bifurcations under certain technical conditions. Double zero bifurcations in power system examples have been analyzed in [6,7].

The other type of codimension two bifurcation studied is a degenerate form of Hopf bifurcation denoted  $B_H^0$  where the cubic normal form coefficient  $a$  becomes zero. Bifurcation theory [1,2] predicts the existence of nested limit cycles in the vicinity of  $B_H^0$  and we illustrate the same in the paper.

In this paper, we study the dynamics of a simple yet fundamental SMIB model through phase portraits and Hopf normal form analysis. Previously in [8], we studied a similar model and showed the existence of hardlimit induced stable limit cycles and hardlimit induced chaos in a similar model. In this paper, we study the problem of when stable limit cycles unrelated to hardlimits, may exist.

## 2. A simple power system model

We consider a single-machine-infinite-bus power system whose dynamics is represented by a simple model shown below that is commonly used in the literature:

$$\dot{\mathbf{d}} = 2\mathbf{p}_0^* \mathbf{w} \quad (1)$$

$$M\dot{\mathbf{w}} = -D\mathbf{w} + P_T - P_G \quad (2)$$

$$T_{d0}\dot{E}' = -(x_d + x)E'/(x_d' + x) + (x_d - x_d')\cos\mathbf{d}/(x_d' + x) + E_{fd} \quad (3)$$

$$T_A\dot{E}_{fd} = -K_A(V - V_{ref}) - (E_{fd} - E_{fd0}) \quad (4)$$

where

$$\begin{aligned} P_G &= E_d I_d + E_q I_q & V &= \sqrt{E_d^2 + E_q^2} \\ E_d &= \frac{X_q \sin \mathbf{d}}{X + X_q} & E_q &= \frac{X E' + X_d' \cos \mathbf{d}}{X + X_d'} \\ I_d &= \frac{E' - E_q}{X_d'} & I_q &= \frac{E_d}{X_q} \end{aligned}$$

In the model, equations (1) and (2) represent the electromechanics. Equation (3) simplifies the electromagnetics in the form of a single axis flux decay equation, and equation (4) is a first order delay type field voltage control.

Here  $V$  stands for the generator terminal bus voltage;  $P_G$  and  $Q_G$  are the real and reactive power outputs of the generator;  $\mathbf{d}$  is the internal rotor angle;  $\mathbf{w}$  is the speed deviation in per unit. The state space for the power system model now consists of four variables  $\mathbf{d}$ ,  $\mathbf{w}$ ,  $E'$ , and  $E_{fd}$ . Among the parameters, the synchronous machine parameters  $M$ ,  $X_d$ ,  $X_q$ , and  $X_d'$  do not vary during system operation. So in our study, they are specified as  $M = 2 * H = 10$  sec.,  $X_d = X_q = 1.0$ , and  $X_d' = 0.2$ . Also, we assume that the damping constant  $D = 1$  pu.

Among the remaining parameters, we study the locus of Hopf bifurcations by varying two parameters at a time. The steady state real power output  $P_T$  is taken as one parameter while the other parameter is one of  $K_A$ ,  $T_A$ ,  $X$ ,  $T_{d0}'$ , and  $V_{ref}$ . The parameters  $P_T$  and  $V_{ref}$  are the real power and nominal bus voltage setting of the generator and these two are true operating parameters.  $K_A$  and  $T_A$  are exciter control parameters that depend on the type of control system used. Even though  $T_{d0}'$  is a machine parameter, we study variations in  $T_{d0}'$  since it is seen to be a sensitive parameter in determining the nonlinear properties of the Hopf bifurcation. Line reactance  $X$  models the static power transfer capacity of the SMIB power system. For a high gain fast exciter controls which are commonly used, the bus terminal voltage  $V$  will be close to the voltage reference setting  $V_{ref}$  from Equation (4). Therefore, as discussed in power system text books, the maximum real power that can be transferred from the generator to the infinite bus is limited by  $V_{ref} / X$ . The higher the values for reactance  $X$ , the more stressed the SMIB system is.

### 3. Study of Hopf bifurcations

In the following figures, dashed lines represent subcritical Hopf bifurcations while solid lines represents supercritical bifurcations. The Hopf coefficient  $\mathbf{a}$  is computed along the Hopf bifurcation locus using a Matlab routine presented in [9].  $B_H^0$  is the transition point where the cubic normal Hopf coefficient  $\mathbf{a}$  equals zero. It can be analyzed by computing the sign of a fifth order normal form coefficient  $a_5$ , and a brief discussion of the codimension two bifurcation  $B_H^0$  follows later.

As stated earlier, our primary interest is on the study of supercritical Hopf bifurcations in the model. In our simulations, we found that the Hopf bifurcations are mostly subcritical. Supercritical Hopf bifurcations could be found only under the conditions of 1) high control gain  $K_A$ , 2) fast exciter control i.e. small  $T_A$ , and 3) large Thevenin reactance  $X$ , and small generator time-constant  $T_{d0}'$ . The parameters are varied accordingly to study transitions from and around supercritical Hopf bifurcations.

In all the plots, the Hopf bifurcation locus  $B_H$  divides the parameter space into two regions: 1) The region to the left of  $B_H$  is denoted "stable" where the equilibrium point is locally stable, and 2) the region to the right of the  $B_H$  is denoted "unstable" where the equilibrium is locally unstable.

All the remaining parameters assume the parameters  $T_{d0}' = 6$ ,  $T_A = 0.01$ ,  $K_A = 1000$ , and  $V_{ref} = 1.05$  unless as stated otherwise. Figure 1 shows the Hopf bifurcation locus for  $(P_T, K_A)$  variation. There are two different types of behavior, for small gain values roughly,  $K_A$  less than 100, and larger gain  $K_A$  values. For small  $K_A$ , the Hopf bifurcation occurs at lower  $P_T$  values when  $K_A$  increases. On the other hand, for gains over 100, the Hopf bifurcation occurs at higher  $P_T$  values when  $K_A$  is increased and the equilibrium is small-signal stable over larger values of  $P_T$ . Moreover, the bifurcation is supercritical only for large  $K_A$  and large  $X$ . We can expect that stable limit cycles will be present surrounding the unstable equilibria for parameter values near the Hopf bifurcation locus in Figure 1.

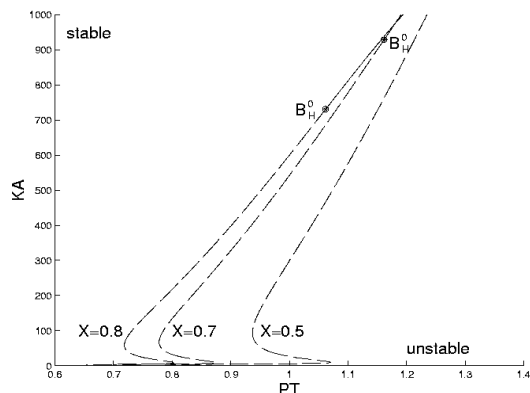


Figure1. Hopf bifurcation locus of  $(P_T, K_A)$

Figure 2 shows Hopf bifurcation loci when  $P_T$  and  $T_A$  are varied. As  $T_A$  becomes smaller, the exciter control is faster and the equilibrium becomes remains stable over larger values of  $P_T$ . We can see from Figure 2 that Hopf bifurcation is supercritical only when  $X$  is large and the time-constant  $T_A$  is small.

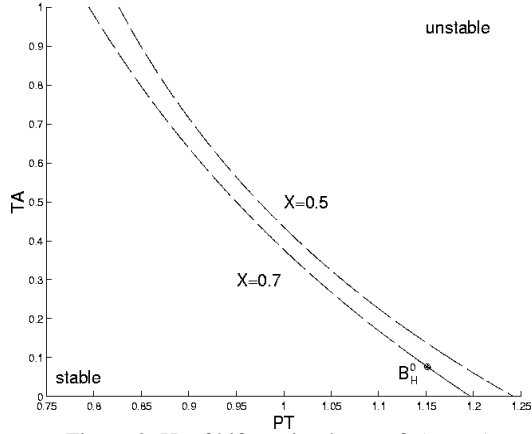


Figure 2. Hopf bifurcation locus of  $(P_T, T_A)$

Figure 3 shows Hopf bifurcations as we vary  $P_T$  and  $V_{ref}$ . The Hopf bifurcations occurs later in  $P_T$ , when  $V_{ref}$  becomes larger. Moreover,  $V_{ref}$  is seen to be insensitive to the sign of the Hopf coefficient  $a$ .

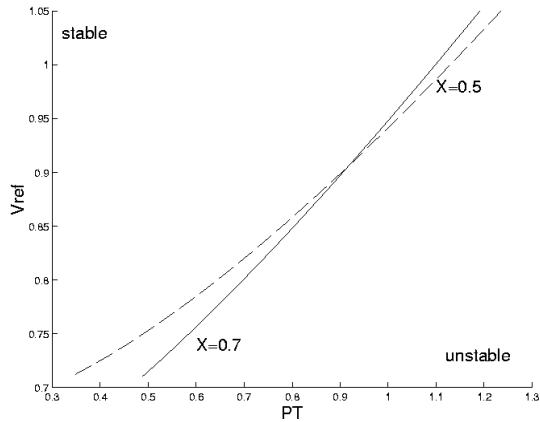


Figure 3. Hopf bifurcation locus of  $(P_T, V_{ref})$

Figure 4 studies variations in  $P_T$  and  $T_{d0}'$ . Hopf bifurcation being a dynamic bifurcation is sensitive to time-constants both in terms of when it occurs and in determining the nonlinear nature of the bifurcation.

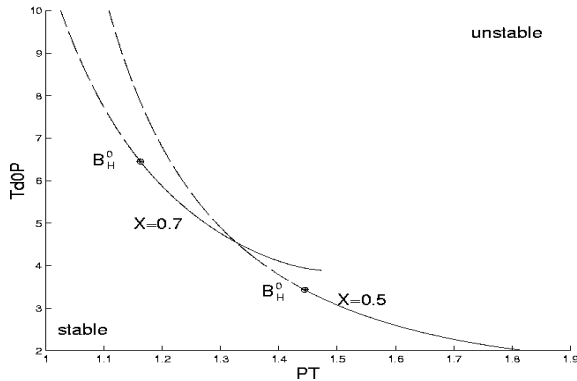


Figure 4. Hopf bifurcation locus of  $(P_T, T_{d0}')$

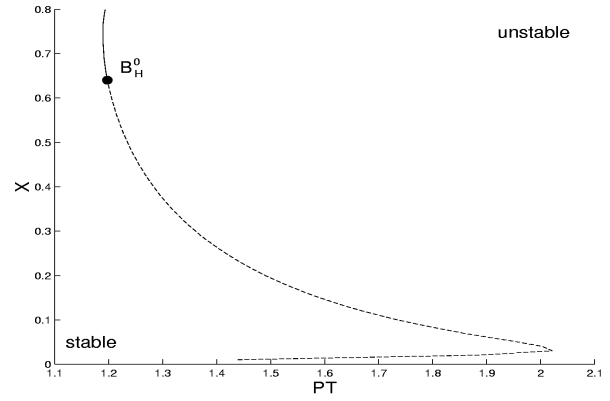


Figure 5. Hopf bifurcation locus of  $(P_T, X)$

Figure 5 shows Hopf bifurcations for variations in  $P_T$  and  $X$ . Excepting for very small values of  $X$ , the Hopf bifurcation occurs at smaller  $P_T$  values when  $X$  increases. As stated earlier, the saddle node bifurcation or the static limit that occurs approximately at  $V_{ref}/X$ , is inversely proportional to  $X$ . For larger  $X$  values above 0.8 (not shown in Figure 5), Hopf bifurcation locus intersects the saddle node bifurcation locus at a codimension two, double zero bifurcation  $B_{DZ}$ . We will study the qualitative system features near the codimension two bifurcations, namely, the degenerate Hopf bifurcation  $B_H^0$ , and the double zero bifurcation  $B_{DZ}$  in the next section.

In summary, we observe that the Hopf bifurcations in the simple SMIB model (1)-(4) are mostly subcritical. Supercritical bifurcations and stable limit cycles do exist when the exciter control is a fast high gain control and when the system is stressed in the form of large line reactance  $X$ .

#### 4. Study of Codimension two bifurcations

##### 4.1 Double Zero bifurcation $B_{DZ}$ :

Hopf bifurcation locus  $B_H$  intersects the saddle node bifurcation locus  $B_{SN}$  at the  $B_{DZ}$  bifurcation in Figure 6. The system Jacobian has a double zero eigenvalue at the  $B_{DZ}$  bifurcation, and the remaining two eigenvalues have negative real parts. By analyzing the quadratic normal form of the vector field at the  $B_{DZ}$  bifurcation point, the presence of homoclinic orbits along a saddle connection bifurcation locus  $B_{SC}$  can be proved [1,2]. Figure 6 shows the bifurcation loci computed numerically for our model. In Figure 6, stable limit cycles born from the supercritical Hopf bifurcations along  $B_H$  are annihilated along the saddle connection bifurcation locus  $B_{SC}$  by colliding with a saddle point that is nearby. The existence of such homoclinic orbits which are attracting trajectories from the unstable focus inside the homoclinic orbit is interesting in the context of complicated nonlinear phenomena. It is interesting to note that the homoclinic orbits along  $B_{SC}$  exist over a rather large range of  $P_T$  and  $X$  values. The implications of homoclinic orbits will be studied in a future paper.

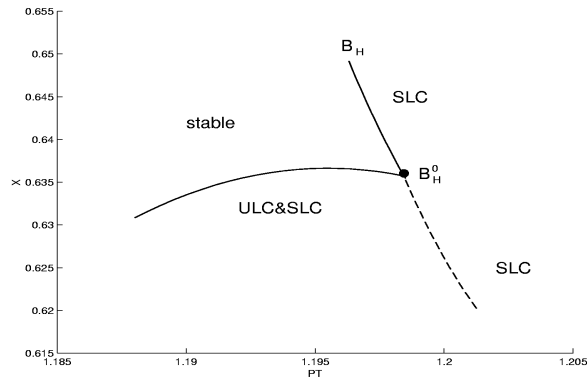


Figure 6. Bifurcation diagram near  $B_{DZ}$  for parameter variations in  $P_T$  and  $X$

#### 4.2 Degenerate Hopf bifurcation $B_H^0$ :

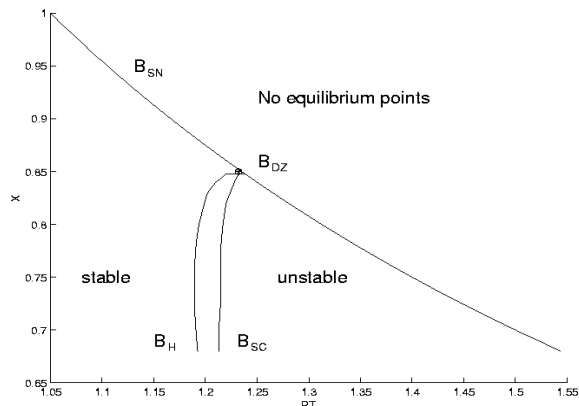


Figure 7. Bifurcation diagram near  $B_H^0$  for parameter variations in  $P_T$  and  $X$

The Hopf bifurcation changes from supercritical Hopf to subcritical Hopf at the  $B_H^0$  bifurcation point in Figure 7. In other words, the Hopf cubic normal form coefficient  $a$  is zero at  $B_H^0$ . By analyzing the fifth order normal form at the bifurcation point, it can be proved that nested limit cycles are present for some parameter values near  $B_H^0$  and the sign of the fifth order normal form coefficient  $a_5$  will determine whether the stable limit cycles surround and dominate over the unstable limit cycles (when  $a_5 < 0$ ) or vice versa. Figure 7 shows the actual bifurcation diagram for our model that has been computed numerically.

From Figure 7, the fifth order coefficient  $a_5$  appears to be negative. Accordingly, when the Hopf bifurcation is supercritical ( $B_H$  above  $B_H^0$  in Figure 7), stable limit cycles are born at  $B_H$  when  $P_T$  increases above  $B_H$ . For a normal subcritical Hopf bifurcation, we expect unstable limit cycles (ULC's) to exist surrounding the stable equilibrium for  $P_T$  near  $B_H^0$ . On the other hand, for parameters near  $B_H^0$ , when  $a_5 < 0$ , both stable and unstable limit cycles exist near  $B_H$  for  $P_T$  less than  $B_H$  values. Stable and unstable limit cycles are born along the global bifurcations called the cyclic fold bifurcations  $B_F$ , and the unstable limit cycles are annihilated at the subcritical Hopf bifurcations. The stable limit cycles

(SLC's) persist on both sides of the subcritical Hopf bifurcation locus for  $B_H$  below  $B_H^0$  in Figure 7. Specifically, in the region bounded by the cyclic fold bifurcations  $B_F$  and  $B_H$  in Figure 7, SLC's of larger size surround ULC's of smaller size. The stable manifold of the ULC separates the regions of attractions of the stable equilibrium point and of the SLC. Therefore, for parameter values in this region, if a postfault initial condition is outside the stability boundary of the stable equilibrium anchored by ULC, then the transient may still converge to the SLC leading to sustained oscillations. An example of the stable limit cycle (SLC) surrounding the unstable limit cycle (ULC) is shown in Figure 8.

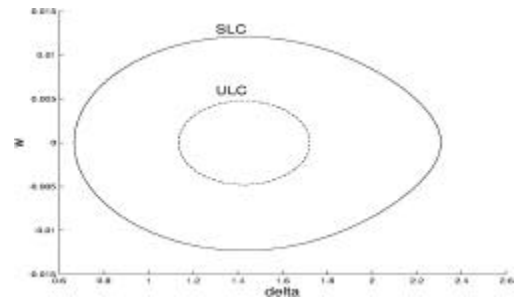


Figure 8. Example of nested limit cycles at  $P_T = 1.195$  and  $X = 0.635$ .

## 5. Conclusions

The paper analyzes the nonlinear nature of Hopf bifurcations in a simple power system model. The paper identifies parametric conditions when the Hopf bifurcation is supercritical. Occurrence and implications of two degenerate bifurcations are studied. Presence of homoclinic orbits and nested limit cycles in the model are observed.

### References:

- [1] J. Guckenheimer, Philip Holmes, "Nonlinear Oscillations, Dynamical Systems, and Bifurcations of Vector Fields", Springer-verlag, New York, 1983.
- [2] S. Wiggins, "Introduction to applied nonlinear dynamical systems and chaos", Springer-Verlag, New York, 1990.
- [3] E. H. Abed and P. P. Varaiya, "Nonlinear oscillations in power systems", International Journal on Electric Power and Energy Systems, Vol. 6, 1984, pp. 37-43.
- [4] H. G. Kwatny, A. K. Pasrija and L. Y. Bahar, "Static bifurcation in power networks: loss of steady state stability and voltage collapse", IEEE Trans. CSAS, Vol. CAS-33, No. 10, October 1986, pp. 981-991.
- [5] C. Rajagopalan, P. W. Sauer, and M. A. Pai, "Analysis of Voltage Control System Exhibiting Hopf Bifurcation", Proceedings of the 28<sup>th</sup> IEEE Conference on Decision and Control, Tampa, Florida, Dec. 1989, pp. 332- 335.

[6] V. Venkatasubramanian, H. Schattler, and J. Zaborszky, "Voltage dynamics: study of a generator with voltage control, transmission and matched MW load", IEEE Trans. Automatic Control, November 1992, pp. 1717-1733.

[7] V. Venkatasubramanian, H. Schattler and J. Zaborszky, "Homoclinic orbits and the persistence of the saddle connection bifurcation for the large electric power system", Proceedings of the International Symposium on Circuits and Systems, 1993.

[8] W. Ji and V. Venkatasubramanian, "Hard-limit induced chaos in a fundamental power system model", International Journal of Electrical Power and Energy Systems, Vol. 18, No.5, September 1996, pp. 279-295.

[9] W. Ji, "Analysis of complicated oscillatory instability phenomena in general power system models", Ph.d. thesis, Washington State University, August 1997.